# Quantum metrology at the limit with extremal Majorana constellations

F. Bouchard,[1] P. de la Hoz,[2] G. Björk,[3] R. W. Boyd,[1,4] M. Grassl,[5,6] Z. Hradil,[7]
E. Karimi,[1,8] A. B. Klimov,[9] G. Leuchs,[5,6,1] J. Řeháček,[7] and L. L. Sánchez-Soto[2,5]

[1]*Department of Physics, University of Ottawa, 150 Louis Pasteur, Ottawa, Ontario, K1N 6N5 Canada*
[2]*Department of Optics, Faculty of Physics, Universidad Complutense, 28040 Madrid, Spain*
[3]*Department of Applied Physics, Royal Institute of Technology (KTH), AlbaNova, SE-106 91 Stockholm, Sweden*
[4]*Institute of Optics, University of Rochester, Rochester, New York, 14627, USA*
[5]*Max Planck Institut for the Science of Light, Staudtstraße 2, 91058 Erlangen, Germany*
[6]*Department of Physics, University of Erlangen-Nuremberg, Staudtstraße 7 B2, 91058 Erlangen, Germany*
[7]*Department of Optics, Palacký University, 17. listopadu 12, 771 46 Olomouc, Czech Republic*
[8]*Department of Physics, Institute for Advanced Studies in Basic Sciences, 45137-66731 Zanjan, Iran*
[9]*Department of Physics, Universidad de Guadalajara, 44420 Guadalajara, Jalisco, Mexico*



**Quantum metrology allows for a tremendous boost in the accuracy of measurement of diverse physical parameters [1]. The estimation of a rotation constitutes a remarkable example of this quantum-enhanced precision [2], and it has been demonstrated in, e.g., magnetometry [3–5] and polarimetry [6, 7]. When the rotation axis is known, NOON states [8] are optimal for this task, achieving a Heisenberg-limit scaling [9]. On the other hand, when the axis is unknown, we show that the optimal states are the recently introduced Kings of Quantumness [10, 11]. We consider the problem in terms of the Majorana stellar representation [12]. The Majorana constellation of NOON states consists of points equidistantly placed around the equator of the Bloch sphere, whereas for the Kings it consists of points uniformly distributed over the sphere. Here, we report the experimental realization of these states by generating up to 21-dimensional orbital angular momentum states of single photons, and confirm their superior sensitivity for measuring a rotation about an arbitrary axis. Our demonstration introduces a new, versatile platform for quantum metrology.**

The conventional description of the quantum world involves a key mathematical object—the quantum state—that conveys complete information about the system under study: once it is known, the probabilities of the outcomes of any measurement can be predicted. This statistical description entails many counterintuitive effects that have prompted several notions of quantumness, yet no single one captures the whole breadth of the physics. Roughly speaking, all hinge on the fact that some properties of the state inherently depend on the Planck constant $h$, which marks a fundamental difference with any classical description.

There are, however, instances of quantum states that behave in an almost classical way. The paradigm of such a behavior is that of coherent states of light [13]: they are as much localized as possible in phase space, a property that is preserved under free evolution.

The concept of coherent states has been extended to other physical systems [14]. The case of a spin is of paramount importance. The corresponding spin coherent states have minimal uncertainty and they are conserved under rotations. So, in the usual way of speaking, they mimic a classical angular momentum as much as possible. One could rightly wonder what kind of state might serve as the opposite of a coherent state. The answer will depend on the ways to formalize the idea of being "the opposite". Here, we take advantage of the Majorana representation, which maps a pure spin $S$ into $2S$ points on the Bloch sphere [12].

It turns out that the Majorana representation of a coherent state consists of a single point (with multiplicity $2S$). At the opposite extreme, we can imagine states whose Majorana representations are spread uniformly over the sphere. With the appropriate metric, the resulting states are precisely the Kings of Quantumness. With such symmetric spreadings, the constellations map onto themselves for relatively small rotations around arbitrary axes. This means that they will resolve rotations around any axis approximately equally well. It is the aim of this work, to experimentally demonstrate the generation of these states and to show their potential for quantum metrology.

Let us first set the stage for our experiment. We consider a system that can be described in terms of two independent bosonic modes, with creation operators $\hat{a}^\dagger_\alpha$, with $\alpha \in \{+,-\}$. This encompasses many different instances, such as strongly correlated systems, light polarization, Bose-Einstein condensates, and Gaussian-Schell beams, to mention only but a few [15]. As it is well known, $\hat{\mathbf{S}} = \frac{1}{2}\hat{a}^\dagger_\alpha \boldsymbol{\sigma}_{\alpha\beta}\,\hat{a}_\beta$, where $\boldsymbol{\sigma}$ are the Pauli matrices and summation over repeated indices is assumed, are the Stokes operators [16], whereas $\hat{N} = \hat{a}^\dagger_\alpha \delta_{\alpha\beta}\,\hat{a}_\beta$ represents the operator for the total number of excitations. In what follows, we restrict our attention to the case where the excitation of $N = N_+ + N_-$ is fixed, with $N_\pm$ being the excitations in each individual mode. These assumptions correspond to working in a $(2S+1)$-dimensional Hilbert space $\mathcal{H}_S$ of spin $S$ (with $N = 2S$). This space $\mathcal{H}_S$ is spanned by the Dicke basis $|S, m\rangle$, wherein the action of $\hat{\mathbf{S}}$ operators is the standard for an angular momentum. Sometimes, it is preferable to use the two-mode Fock basis $|N_+, N_-\rangle$; it is related to the Dicke basis by the substitutions $N_+ = S + m$ and $N_- = S - m$.

Spin coherent states are constructed much in the same way as in the canonical case: they are displaced versions of the north pole of the Bloch unit sphere $\mathcal{S}_2$. If $\mathbf{n}$ is a unit vec-

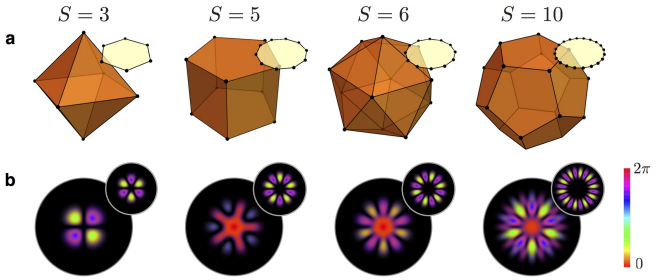


FIG. 1. **Visualisation of Kings constellations. a,** The Majorana constellations in the Bloch sphere for the Kings (orange) and the NOON states (yellow) corresponding to spin $S = 3, 5, 6$, and 10. **b,** The Laguerre-Gauss representation of the same Kings and NOON states, shown in **a**, where the azimuthal index $\ell$ corresponds to $m$ in the Dicke basis. We consider the fundamental radial mode; i.e., $p = 0$, where $p$ is the radial index of the Laguerre-Gauss modes.

tor in the direction of the spherical angles $(\theta, \phi)$, they can be defined as $|\mathbf{n}\rangle = e^{i\phi\hat{S}_z} e^{i\theta\hat{S}_y} |S, S\rangle$. They are not orthogonal: $\langle \mathbf{n}_1 | \mathbf{n}_2 \rangle = [(1 + \mathbf{n}_1 \cdot \mathbf{n}_2)/2]^S \exp[i\Phi(\mathbf{n}_1, \mathbf{n}_2)]$, with $\Phi(\mathbf{n}_1, \mathbf{n}_2)$ the area of the geodesical triangle on $\mathcal{S}_2$ with the vertices at the north pole, $\mathbf{n}_1$ and $\mathbf{n}_2$. However, they are a complete system that allows for a resolution of the identity. In particular, one can decompose an arbitrary state $|\Psi\rangle$ using this basis. The associated coherent-state wave function is $\Psi(\mathbf{n}) = \langle \mathbf{n} | \Psi \rangle$, and the corresponding probability distribution, $Q(\mathbf{n}) = |\Psi(\mathbf{n})|^2$, is nothing but the Husimi function. The wave function $\Psi(\mathbf{n})$ can be expanded in terms of the Dicke basis $|S, m\rangle$. If we denote the corresponding expansion coefficients by $\Psi_m = \langle S, m | \Psi \rangle$, we obtain $\Psi(\mathbf{n}) = (1 + |z|^2)^{-S} \sum_{m=-S}^{S} c_m \Psi_m z^{S+m}$, where $c_m = \sqrt{(2S)!/[(S-m)!(S+m)!]}$ and $z = \tan(\theta/2) e^{-i\phi}$ is the complex number derived by the stereographic projection of $(\theta, \phi)$. Apart from the unessential positive prefactor, this is a polynomial of order $2S$; thus, $|\Psi\rangle$ is determined by the set $\{z_i\}$ of the $2S$ complex zeros of $\Psi(\mathbf{n})$. These zeros, which are also the zeros of $Q(\mathbf{n})$, specify the so-called constellation by an inverse stereographic map of $\{z_i\} \mapsto \{\theta_i, \phi_i\}$.

Since the spherical harmonics are a complete set of orthonormal functions on $\mathcal{S}_2$, they may be used to expand the Husimi function $Q(\mathbf{n})$; the resulting coefficients are

$$\varrho_{Kq} = C_K \int_{\mathcal{S}_2} d^2\mathbf{n}\, Y_{Kq}(\mathbf{n})\, Q(\mathbf{n}), \qquad (1)$$

where $C_K$ is just a normalization constant. Actually, the $\varrho_{Kq}$ are nothing but the standard state multipoles [17] and there are $2S + 1$ of them. When expressed in the Cartesian basis they appear in a very transparent way. For example, the dipole ($\varrho_{1q}$) and the quadrupole ($\varrho_{2q}$) terms can be given as $\wp_i = \langle n_i \rangle$ and $\mathcal{Q}_{ij} = \langle 3n_i n_j - \delta_{ij} \rangle$, respectively, where $\langle f(\mathbf{n}) \rangle = \int_{\mathcal{S}_2} d^2\mathbf{n}\, f(\mathbf{n})\, Q(\mathbf{n}) / \int_{\mathcal{S}_2} d^2\mathbf{n}\, Q(\mathbf{n})$ and the index $i$ runs $x, y$, and z. These multipoles appear then as the standard ones in electrostatics, but replacing the charge density by $Q(\mathbf{n})$ and distances by directions. It is also clear that they are the $K$th directional moments of the state constellation and, therefore, these terms resolve progressively finer angular features.

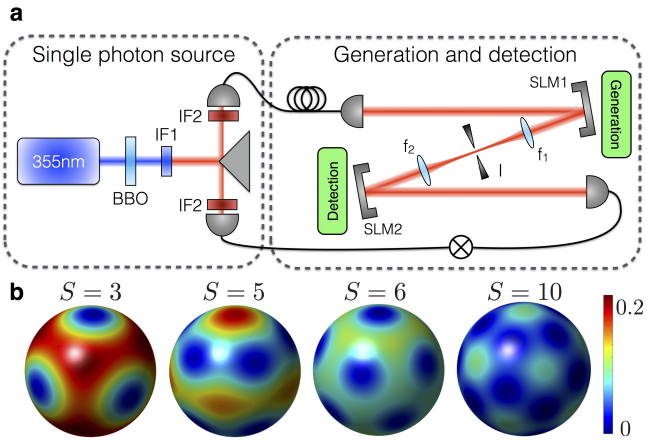


FIG. 2. **Sketch of the experimental setup and measured Husimi $Q$ functions. a,** Single photons created by spontaneous parametric downconversion i a $\beta$-barium borate (BBO) crystal are separated from one another and coupled into single-mode fibres, where interference filters (IF) are placed in the paths of the photons. One of the photons impinges on a spatial light modulator (SLM1), where a hologram is displayed to generate the desired phase and intensity profile of the Kings. The generated state is projected onto a second state using another spatial light modulator (SLM2) to measure the overlap of the two states. **b,** Density plots of the experimentally reconstructed Husimi $Q$ functions for the same King states as in Fig. 1. The fidelities of these reconstructed states are (from left to right) 0.94, 0.87, 0.91, and 0.93. The differences with the theoretical $Q$ functions cannot be visually noticed.

The dipole indicates the position of the state in the Bloch sphere. When $\wp$ vanishes, the state has vanishing (first-order) polarization and points nowhere in the mean: in this way, it serves as the opposite of a state that points, as much as possible, somewhere. If the quadrupole also vanishes, the variance of the state is uniform; i.e., no directional signature can be observed in its second-order fluctuations and we say that it is second-order unpolarized. Similar interpretation holds for higher-order multipoles. The quantity $\sum_q |\varrho_{Kq}|^2$ gauges the overlap of the state with the $K$th multipole pattern. It seems thus suitable to look at the cumulative distribution [18] $\mathcal{A}_M = \sum_{K=1}^{M} \sum_{q=-K}^{K} |\varrho_{Kq}|^2$, which concisely condenses the state angular capacity up to order $M$ ($1 \le M \le 2S$). Observe that the monopole is omitted, as it is just a constant term.

The spin coherent states $|\mathbf{n}\rangle$ have remarkably simple constellations, just the point $-\mathbf{n}$, and maximize $\mathcal{A}_M$ for all orders $M$, confirming yet from another perspective the outstanding properties of these states [10]. In contradistinction, the Kings are those pure states that make $\mathcal{A}_M \equiv 0$ for the highest possible value of $M$. This means that they convey the relevant information in higher-order fluctuations. The search for these states has been systematically undertaken recently in Ref. [10], where the interested reader can check the details (see also Methods). The resulting Majorana constellations for some values of $S$ are depicted in Fig. 1. For $S = 3$, the constellation is a regular octahedron and the state is third-order unpolarized ($M = 3$). For $S = 5$, it consists of two pentagons.

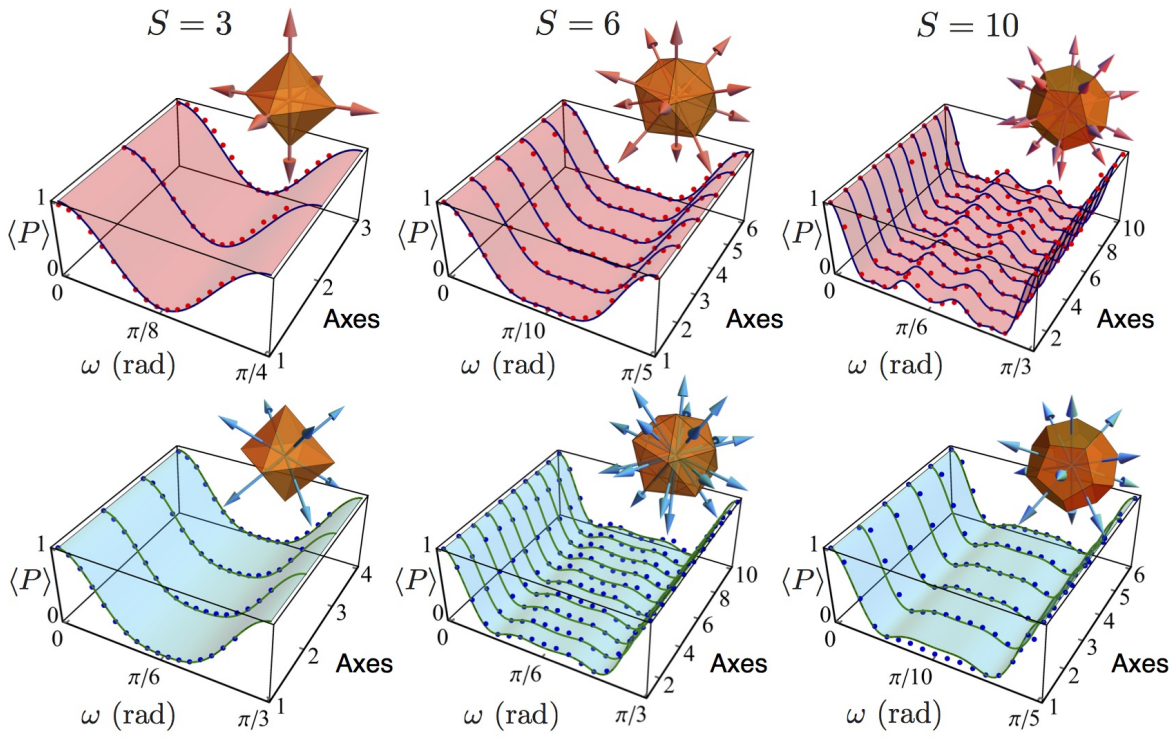


FIG. 3. **Kings sensitivity for rotation estimation.** Experimental results of the projection of the $S = 3, 6$ and 10 (first, second and third column respectively) Kings states, $|\Psi^{(S)}\rangle$, onto themselves after a rotation of $\omega$, $\hat{R}(\omega)$, i.e. $\langle\hat{P}\rangle = \left|\langle\Psi^{(S)}|\hat{R}(\omega)|\Psi^{(S)}\rangle\right|^2$. The axes are presented graphically along with the associated constellations. The first row corresponds to rotations along the axes passing through the Majorana points (pink arrows) and the second row corresponds to rotations along the axes normal to the facets of the constellations (blue arrows). The experimental results (red and blue dots) are shown along with the theoretical results (blue and green curves) for all rotation axes.

For $S = 6$ we have the icosahedron, and the corresponding state is fifth-order unpolarized. For $S = 10$ we have a slightly stretched dodecahedron (i.e., the four pentagonal rings that define its vertices are displaced against the pole) and it is fifth-order unpolarized. Accordingly, the Kings have the points as symmetrically placed on the unit sphere as possible. Their constellations possess then many axes along which they return to themselves after a small rotation. Consequently, they can resolve relatively small angles around a large number of axes.

Other states with a high degree of angular resolution are the NOON states, given by $|\text{NOON}\rangle = \frac{1}{\sqrt{2}}(|N,0\rangle - |0,N\rangle)$ in the two-mode Fock basis and $\frac{1}{\sqrt{2}}(|S,S\rangle - |S,-S\rangle)$ in the Dicke basis. As shown in Fig. 1 their Majorana constellation consists of $2S$ equidistantly placed points around the equator of $\mathcal{S}_2$. A rotation around the $z$ axis of angle $\pi/(2S)$ makes $|\text{NOON}\rangle$ ortogonal to itself, whereas for $\pi/S$ it returns to itself. This nicely supports the ability of NOON states to detect small rotations.

To compare the performance of these two classes of states, let us assume we have to estimate a rotation $R(\omega, \mathbf{u})$ of angle $\omega$ around an axis $\mathbf{u}$ of spherical angles $(\Theta, \Phi)$. We take the measurement to be a projection of the rotated state onto the original one; i.e., it can be represented by $\hat{P} = |\Psi\rangle\langle\Psi|$. The sensitivity of a state $|\Psi\rangle$ to this measurement can be retrieved from simple error propagation [19]

$$\Delta\omega = \frac{\Delta\hat{P}}{\left|\partial\langle\hat{P}\rangle/\partial\omega\right|}, \tag{2}$$

where $\Delta\hat{P} = [\langle\hat{P}^2\rangle - \langle\hat{P}\rangle^2]^{1/2}$. The final results are (see Methods)

$$\Delta\omega_{\text{Kings}} = \frac{\sqrt{3}}{\sqrt{2}}\frac{1}{\sqrt{S(S+1)}},$$
$$\Delta\omega_{\text{NOON}} = \frac{1}{\sqrt{2}}\frac{1}{\sqrt{2S^2\cos^2\Theta + S\sin^2\Theta}}. \tag{3}$$

The sensitivity of the Kings is completely independent of the rotation axis and with a Heisenberg-limit scaling $1/S$ for large $S$. On the contrary, for the NOON states, only when $\Theta = 0$ (i.e. the rotation is about the $z$ axis) we recover the optimal scaling $1/S$. In short, it is essential to know the rotation axis to ensure that the NOON state is aligned to achieve its best sensitivity. Note, however, that the measurement scheme for $\Delta\omega$ involves only second-order moments of $\hat{\mathbf{S}}$. Given their properties, one could expect that detecting higher-order moments will bring out even more advantages of the Kings.

To check these issues we have generated these extremal states for the cases of $S = 3, 5, 6$ and 10, using orbital angular momentum (OAM) states of single photons [20]. In the

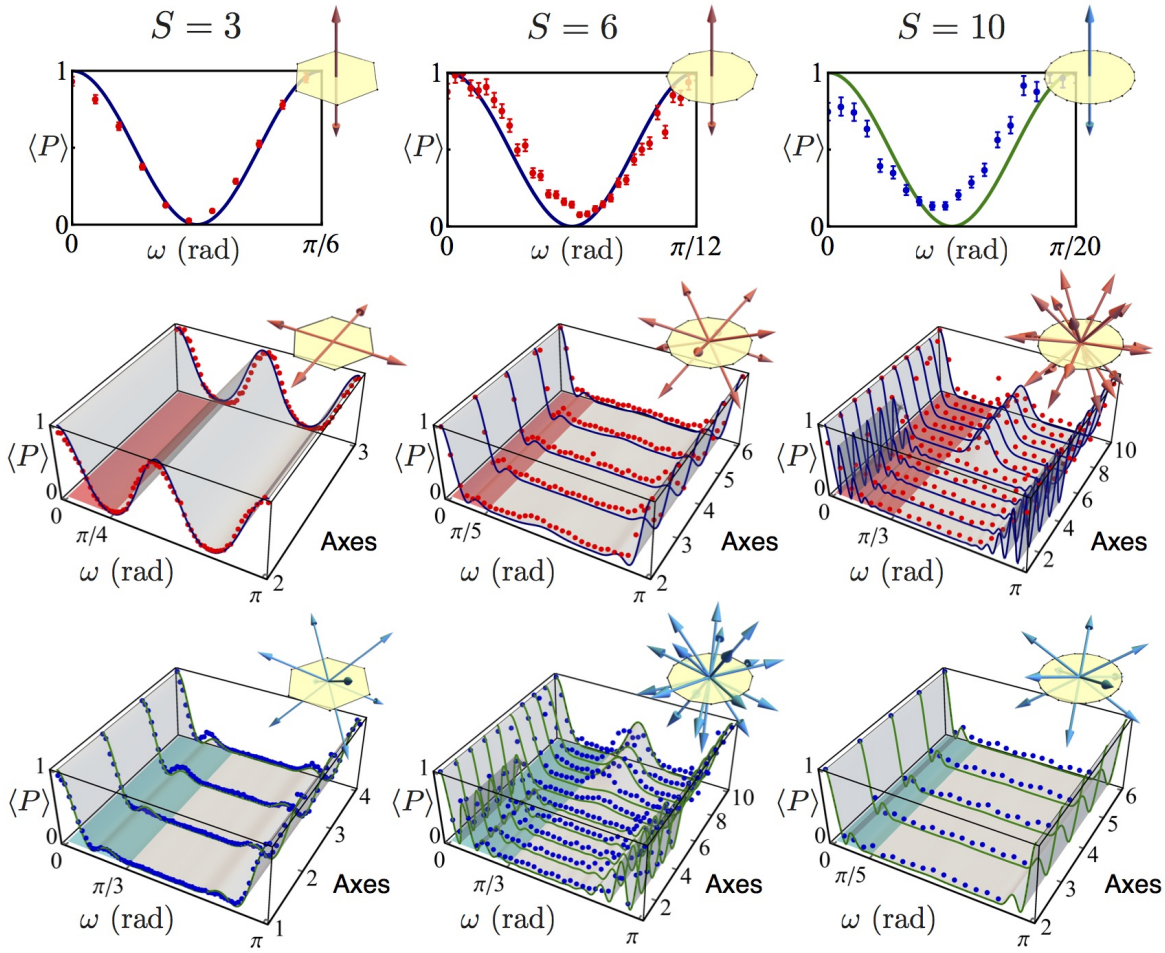


FIG. 4. **Kings superiority over NOON states.** Experimental results of projecting NOON states corresponding to $S = 3, 6$ and 10 onto themselves after a rotation along the various axes sketched in Fig. 3. In the first row, the NOON states are rotated around their optimal $z$ axis. For a comparison of the NOON versus the Kings, we show rotations of the NOON states along the axes of rotation defined by the Majorana points (second row) and the normal to the facets (third row) of the constellations of the Kings with corresponding $S$. The axes are presented graphically along with the associated constellations on the top-right corner of each plot. The coloured region (red for Majorana points rotations and blue for facets rotation) shows the region for which the Kings are mapped back onto themselves, as shown in Fig. 3. Although the drop in $\langle \hat{P} \rangle$ near $\omega = 0$ can be more abrupt for NOON states, the sensitivity in Eq. (2) for Kings states, apart from a single axis rotation (shown in the first row), is much higher than for NOON states.

Dicke basis, the index $m$ is directly related to the OAM value of a single photon along its propagation direction. We used Laguerre-Gauss modes, so in that basis the Kings have the following nonzero $\Psi_m$ components:

$$\begin{array}{l|lll} S=3 & \Psi_{\pm 2} = \mp\frac{1}{\sqrt{2}} & & \\ S=5 & \Psi_{\pm 5} = \frac{1}{\sqrt{5}} & \Psi_0 = \sqrt{\frac{3}{5}} & \\ S=6 & \Psi_{\pm 5} = \mp\frac{\sqrt{7}}{5} & \Psi_0 = \frac{\sqrt{11}}{5} & \\ S=10 & \Psi_{\pm 10} = \frac{\sqrt{561}}{75} & \Psi_{\pm 5} = \mp\frac{3\sqrt{209}}{75} & \Psi_0 = \frac{\sqrt{741}}{75} \end{array} \tag{4}$$

In this Laguerre-Gauss basis, the transverse profiles of both the Kings and the NOON states are as in Fig. 1-**b**.

We experimentally create the Kings at the single-photon regime by means of spontaneous parametric downconversion (see Methods for details). A sketch of the experimental setup is shown in Fig. 2-**a**. The generated photons pairs, namely signal and idler, were spatially cleaned by coupling into single-mode optical fibres. The idler photons are used to herald the signal photons, which are themselves sent to a spatial light modulator (SLM1) to generate the desired quantum states [21]. The generated photonic Kings are subsequently sent to a second spatial light modulator (SLM2) followed by a single mode optical fibre, where they are experimentally analyzed by means of projective measurements [22].

To verify the accurate experimental generation of these states, we perform quantum state tomography to reconstruct the Husimi $Q$ function, as shown in Fig. 2-**b**. In this reconstruction, two different sets of projections were utilized: (i) projections onto coherent states and (ii) projections onto rotated Kings states with the axes of rotations defined by the

Majorana points. We describe such a measurement with an overcomplete set of positive operator-valued measurements $\{\hat{\Pi}_j \geq 0\}$, so the probabilities $p_j$ of observed relative frequencies $f_j$ as given by the Born rule $p_j = \mathrm{Tr}(\varrho\Pi_j)$. A few hundred projections were recorded in each dimension $S = 3, 5, 6$ and 10, from which we estimate the quantum state using standard maximum likelihood techniques. The average fidelity of the resulting states is above 90%; i.e., 94%, 87%, 91% and 93%, respectively.

We now study the behaviour of such states under rotations in the sphere $\mathcal{S}_2$. This is experimentally realized by means of projective measurements of the Kings onto themselves after a rotation $\omega$ around several axes (see Fig. 3). To demonstrate the high sensitivity to rotation of these states along arbitrary axes, we perform such rotations around each axis passing through the Majorana points and facets of the Kings constellations. For the cases of $S = 3, 6$ and 10, we find four-, five- and three-fold symmetry axes passing through their Majorana points and three-, three- and five-fold symmetry axes passing through the normals to the facets of their constellations, respectively.

Finally, in Fig. 4 we experimentally confirm the superiority of the Kings over the NOON states. For this purpose, we have used the case of $S = 3$, 6 and 10, as well. To compare the performances of the NOON states with that of the Kings, we perform the same set of projective measurements by rotating the NOON states over the same axes discussed in previously for the Kings. However, due to their lack of rotation sensitivity, the NOON states are studied under a full rotation of $\pi$. As it was expected, the NOON states possess the largest sensitivity to rotation for a single axis ($z$), thus overcoming the Kings for this case. Nonetheless, it is clearly evident that the Kings are distinctly superior with respect to any other rotation axes.

The problem of the Kings is closely related to other notions as states of maximal Wehrl-Lieb entropy [23], Platonic states [24], the Queens of Quantumness [25] or the Thomson problem [26]. However, there are still many things to elucidate concerning these links. They are though a nice illustration of the connections between different branches of science, and on how some seemingly simple problems—distributing points in the most symmetric manner on a sphere—can illuminate such complicated optimization problems that we have just described.

Thus far, efforts were concentrated in estimating the rotation angle, which in terms of magnetometry means that we only want to know the magnetic field magnitude. The Kings will allow for a simultaneous precise determination of the rotation axis (i.e., the magnetic field direction). Our experimental results corroborate that this extra advantage can pave the way to much more refined measurement schemes.

## Methods

**Extremal states:** The multipoles associated with a state $\hat{\varrho}$ living in the $(2S+1)$-dimensional Hilbert space $\mathcal{H}_S$ of spin $S$ can be defined in terms of the Husimi $Q$ function as

$$\varrho_{Kq} = C_K \int_{\mathcal{S}_2} d^2\mathbf{n}\, Y_{Kq}(\mathbf{n})\, Q(\mathbf{n}), \tag{1}$$

where the normalization constant is $C_K = \sqrt{4\pi/(2S+1)}/C^{SS}_{SS,K0}$ and $C^{SS}_{SS,K0}$ is a Clebsch-Gordan coefficient.

We look at the cumulative distribution

$$\mathcal{A}_M = \sum_{K=1}^{M} \sum_{q=-K}^{K} |\, \varrho_{Kq}\,|^2, \tag{2}$$

which sums polarization information up to order $M$ ($1 \leq M \leq 2S$). The distribution $\mathcal{A}_M$ can be regarded as a nonlinear functional of the density matrix $\hat{\varrho}$. On that account, one can try to ascertain the states that maximize $\mathcal{A}_M$ for each order $M$. As with any cumulative distribution, $\mathcal{A}_M$ is a monotonically nondecreasing function of the multipole order. We shall be considering only pure states, which we expand in the Dicke basis as $|\Psi\rangle = \sum_{m=-S}^{S} \Psi_m |S, m\rangle$, with coefficients $\Psi_m = \langle S, m|\Psi\rangle$. We easily get

$$\mathcal{A}_M = \sum_{K=1}^{M} \sum_{q=-K}^{K} \frac{2K+1}{2S+1} \left| \sum_{m,m'=-S}^{S} C^{Sm'}_{Sm,Kq} \Psi_{m'} \Psi^*_m \right|^2. \tag{3}$$

As it has been proven in Ref. [10], spin coherent states $|\mathbf{n}\rangle$ maximize $\mathcal{A}_M$ for all orders $M$.

We concentrate on the opposite case of states minimizing $\mathcal{A}_M$. Obviously, the maximally mixed state $\hat{\varrho} = \frac{1}{2S+1}\hat{\mathbb{1}}_{2S+1}$ kills all the multipoles and so indeed causes (2) to vanish for all $M$, being fully unpolarized [27, 28]. Nonetheless, we are interested in pure $M$th-order unpolarized states. The strategy we adopt is thus very simple to state: starting from a set of unknown normalized state amplitudes in Eq. (3), which we write as $\Psi_m = a_m + ib_m$ ($a_m, b_m \in \mathbb{R}$), we try to get $\mathcal{A}_M = 0$ for the highest possible $M$. This yields a system of polynomial equations of degree two for $a_m$ and $b_m$, which we solve using Gröbner bases implemented in the computer algebra system MAGMA. In this way, we get exact algebraic expressions and we can detect when there is no feasible solution.

The detailed list of resulting minimal states, which are the Kings of Quantumness, can be found in http://polarization.markus-grassl.de, where the reader can also see the associated Majorana constellations.

Intuitively, these constellations seem to have the points as symmetrically placed on the unit sphere as possible. We have explored the connection with spherical $t$-designs [29], which are patterns of $N$ points on a sphere such that every polynomial of degree at most $t$ has the same average over the $N$ points as over the sphere. Thus, the $N$ points mimic a flat distribution up to order $t$, which obviously implies a fairly symmetric distribution.

For a given $S$, the maximal order of $M$ for which we can cancel out $\mathcal{A}_M$ does not follow a clear pattern. However, the numerical evidence suggests that $M_{\max}$ coincides with $t_{\max}$ in the corresponding spherical design. Further work is needed, however, to support this conjecture.

**Experimental Setup:** A quasi-continuous wave UV laser operating with a repetition rate of 100 MHz and an average power of 150 mW at a wavelength of 355 nm is used to pump a type-I $\beta$-barium borate crystal. The single photons, signal and idler, are subsequently coupled to single mode fibres to filter their spatial mode. One of the photons, the idler, is used as a trigger. The other photon, the signal, is made incident on a first spatial light modulator (SLM1), where the desired quantum states were imprinted on the signal photon holographically. The generated single-photon state is imaged onto a second spatial light modulator (SLM2) by means of a $4f$ system. The second SLM possessing the desired hologram followed by a single mode optical fibre perform the projective measurement on the state of the signal photon. Both photons are sent to avalanche photodiode detectors (APD) and coincidence counts are recorded by means of a coincidence box with a coincidence time window of 3 ns.

**Rotational sensitivity:** The goal of this work is the estimation of a rotation $\hat{R}(\omega, \mathbf{u})$ of angle $\omega$ around an axis $\mathbf{u}$ of spherical angles $(\Theta, \Phi)$. Our measurement was a projection onto the original state; i.e., $\hat{P} = |\Psi\rangle\langle\Psi|$. The sensitivity of the state $|\Psi\rangle$ to this measurement is defined as been defined as

$$\Delta\omega = \frac{\Delta\hat{P}}{\left|\partial\langle\hat{P}\rangle/\partial\omega\right|}. \tag{4}$$

We consider only small rotations, which means that the angle $\omega$ is small enough to expand $\hat{R}(\omega, \mathbf{u})$ up to second order. Obviously, $\langle\hat{P}\rangle = |\langle\Psi|\hat{R}|\Psi\rangle|^2$ and then, after a direct computation, we get

$$\begin{aligned} \langle\hat{P}_{\mathrm{Kings}}\rangle &= 1 - \tfrac{1}{3}\omega^2 S(S+1), \\ \langle\hat{P}_{\mathrm{NOON}}\rangle &= 1 - \tfrac{1}{2}\omega^2 S\left(\sin^2\Theta + \tfrac{1}{2}S\cos^2\Theta\right). \end{aligned} \tag{5}$$

From here we can calculate the denominator in (4). The variance can be obtained along the same lines. The final result is precisely the sensitivity quoted in Eq. (3).

**Tomography:** To verify the generated states two different sets of projections were utilized: (i) projections onto coherent states and (ii) projections onto rotated Kings with the axes of rotations defined by the Majorana points. Such a $D$-dimensional channel can be described by an overcomplete positive operator-valued measurement (POVM) $\hat{\Pi}_j \geq 0, j = 1, \ldots, D$. The probabilities $p_j$ of observed relative frequencies $f_j$, as given by the Born rule $p_j = \mathrm{Tr}(\hat{\varrho}\hat{\Pi}_j)$ can be inverted by maximizing the Fermi extended likelihood

$$\mathcal{L} = \sum_j^D f_j \log\left(\frac{p_j}{\sum_{j'} p_{j'}}\right) \tag{6}$$

to yield the Kings estimates. This amounts to solving the extremal equation

$$\hat{R}\hat{\varrho} = \hat{G}\hat{\varrho}\,, \tag{7}$$

where we have defined

$$\hat{R} = \sum_j \frac{f_j}{p_j(\rho)}\hat{\Pi}_j, \qquad \hat{G} = \frac{\sum_j f_j}{\sum_j p_j(\rho)} \sum_j \hat{\Pi}_j. \tag{8}$$

This can be solved in an iterative way

$$\hat{\varrho}^{(k+1)} = \hat{G}^{-1}\hat{R}\hat{\varrho}^{(k)}\hat{R}\hat{G}^{-1}, \tag{9}$$

starting from the $(2S+1)$-dimensional maximally mixed state $\hat{\varrho} = \frac{1}{2S+1}\hat{\mathbb{1}}_{2S+1}$. A few thousand of iterations are typically needed to observe a convergence to the stationary point of the map (7).

In the experiment, several hundred of projections were recorded for each King and the fidelities of the estimated states with respect to the target states were found to be close to or in excess of 90% in all cases. See Table I for details.

| $S$ | dim | $D$ | fidelity |
|---|---|---|---|
| 3 | 7 | 288 | 0.94 |
| 5 | 11 | 572 | 0.87 |
| 6 | 13 | 544 | 0.91 |
| 10 | 21 | 1054 | 0.93 |

TABLE I. Measurement sizes $D$ and resulting fidelities obtained with quantum state tomography of experimentally generated King states.

**Acknowledgments** F. B. acknowledges the support of the Vanier Canada Graduate Scholarships Program of the Natural Sciences and Engineering Research Council of Canada (NSERC). E. K. acknowledges the support of the Canada Research Chairs (CRC), and Canada Foundation for Innovation (CFI) Programs. F. B., R. W. B and E. K. acknowledge the support of the Max Planck–University of Ottawa Centre for Extreme and Quantum Photonics. Z. H. and J. R. acknowledge the support from the Technology Agency of the Czech Republic (Grant TE01020229), the Grant Agency of the Czech Republic (Grant 15-03194S) and the IGA Project of the Palacký University (Grant IGA PrF 2016-005). A. B. K. acknowledges the Mexican CONACyT (Grant 254127). P. H. and L. L. S. S. acknowledges the support of the Spanish MINECO (Grant FIS2015-67963-P).

**Author Information** The authors declare no competing financial interests. Correspondence and requests for materials should be addressed to E. K. (ekarimi@uottawa.ca) or L. L. S. S. (lsanchez@fis.ucm.es).

[1] Giovannetti, V., Lloyd, S. & Maccone, L. Advances in quantum metrology. *Nat. Photon.* **5**, 222–229 (2011).
[2] Rozema, L. A., Mahler, D. H., Blume-Kohout, R. & Steinberg, A. M. Optimizing the choice of spin-squeezed states for detecting and characterizing quantum processes. *Phys. Rev. X* **4**, 041025 (2014).
[3] Wasilewski, W. *et al.* Quantum noise limited and entanglement-assisted magnetometry. *Phys. Rev. Lett.* **104**, 133601 (2010).
[4] Sewell, R. J. *et al.* Magnetic sensitivity beyond the projection noise limit by spin squeezing. *Phys. Rev. Lett.* **109**, 253605– (2012).
[5] Muessel, W., Strobel, H., Linnemann, D., Hume, D. B. & Oberthaler, M. K. Scalable spin squeezing for quantum-enhanced magnetometry with bose-einstein condensates. *Phys. Rev. Lett.* **113**, 103004 (2014).
[6] Meyer, V. *et al.* Experimental demonstration of entanglement-enhanced rotation angle estimation using trapped ions. *Phys. Rev. Lett.* **86**, 5870–5873 (2001).
[7] D' Ambrosio, V. *et al.* Photonic polarization gears for ultra-sensitive angular measurements. *Nat. Commun.* **4**, 2432 EP – (2013).
[8] Lee, H., Kok, P. & Dowling, J. P. A quantum Rosetta stone for interferometry. *J. Mod. Opt.* **49**, 2325–2338 (2002).
[9] Dowling, J. P. Quantum optical metrology–the lowdown on high-N00N states. *Contemp. Phys.* **49**, 125–143 (2008).
[10] Björk, G. *et al.* Extremal quantum states and their Majorana constellations. *Phys. Rev. A* **92**, 031801 (2015).
[11] Björk, G., Grassl, M., de la Hoz, P., Leuchs, G. & Sánchez-Soto, L. L. Stars of the quantum universe: extremal constellations on the Poincaré sphere. *Physica Scripta* **90**, 108008 (2015).
[12] Majorana, E. Atomi orientati in campo magnetico variabile. *Nuovo Cimento* **9**, 43–50 (1932).
[13] Glauber, R. J. Coherent and incoherent states of radiation field. *Phys. Rev.* **131**, 2766–2788 (1963).
[14] Perelomov, A. *Generalized Coherent States and their Applications* (Springer, Berlin, 1986).
[15] Chaturvedi, S., Marmo, G. & Mukunda, N. The Schwinger representation of a group: concept and applications. *Rev. Math. Phys.* **18**, 887–912 (2006).
[16] Luis, A. & Sánchez-Soto, L. L. Quantum phase difference, phase measurements and Stokes operators. *Prog. Opt.* **41**, 421–481 (2000).
[17] Blum, K. *Density Matrix Theory and Applications* (Plenum, New York, 1981).
[18] de la Hoz, P. *et al.* Multipolar hierarchy of efficient quantum polarization measures. *Phys. Rev. A* **88**, 063803 (2013).
[19] Jha, A. K., Agarwal, G. S. & Boyd, R. W. Supersensitive measurement of angular displacements using entangled photons. *Phys. Rev. A* **83**, 053829 (2011).
[20] Allen, L., Barnett, S. M. & Padgett, M. J. *Optical Angular Momentum* (Institute of Physics Publishing, Bristol, 2003).
[21] Bolduc, E., Bent, N., Santamato, E., Karimi, E. & Boyd, R. W. Exact solution to simultaneous intensity and phase encryption with a single phase-only hologram. *Opt. Lett.* **38**, 3546–3548 (2013).
[22] Qassim, H. *et al.* Limitations to the determination of a Laguerre-Gauss spectrum via projective, phase-flattening measurement. *J. Opt. Soc. Am. B* **31**, A20 (2014).
[23] Baecklund, A. & Bengtsson, I. Four remarks on spin coherent states. *Phys. Scr.* **T163**, 014012 (2014).

[24] Kolenderski, P. & Demkowicz-Dobrzanski, R. Optimal state for keeping reference frames aligned and the platonic solids. *Phys. Rev. A* **78**, 052333 (2008).

[25] Giraud, O., Braun, P. & Braun, D. Quantifying quantumness and the quest for queens of quantumness. *New J. Phys.* **12**, 063005 (2010).

[26] Thomson, J. J. On the structure of the atom: an investigation of the stability and periods of oscillation of a number of corpuscles arranged at equal intervals around the circumference of a circle; with application of the results to the theory of atomic structure. *Philos. Mag. Ser. 6* **7**, 37265 (1904).

[27] Prakash, H. & Chandra, N. Density operator of unpolarized radiation. *Phys. Rev. A* **4**, 796–799 (1971).

[28] Agarwal, G. S. On the state of unpolarized radiation. *Lett. Nuovo Cimento* **1**, 53–56 (1971).

[29] Delsarte, P., Goethals, J. M. & Seidel, J. J. Spherical codes and designs. *Geom. Dedicata* **6**, 363–388 (1977).